

Primary energy reconstruction at KASCADE-Grande using the S(500) method

G. TOMA⁵, W.D. APEL¹, J.C. ARTEAGA-VELÁZQUEZ², K. BEKK¹, M. BERTAINA³, J. BLÜMER^{1,4}, H. BOZDOĞ¹, I.M. BRANCUS⁵, E. CANTONI^{3,6,a}, A. CHIAVASSA³, F. COSSAVELLA^{4,b}, C. CURCIO³, K. DAUMILLER¹, V. DE SOUZA⁷, F. DI PIERRO³, P. DOLL¹, R. ENGEL¹, J. ENGLER¹, B. FUCHS⁴, D. FUHRMANN^{8,c}, A. GHERGHEL-LASCU⁵, H.J. GILS¹, R. GLASSTETTER⁸, C. GRUPEN⁹, A. HAUNGS¹, D. HECK¹, J.R. HÖRANDEL¹⁰, D. HUBER⁴, T. HUEGE¹, K.-H. KAMPERT⁸, D. KANG⁴, H.O. KLAGES¹, K. LINK⁴, P. ŁUCZAK¹¹, M. LUDWIG⁴, H.J. MATHES¹, H.J. MAYER¹, M. MELISSAS⁴, J. MILKE¹, B. MITRICA⁵, C. MORELLO⁶, J. OEHLISCHLÄGER¹, S. OSTAPCHENKO^{1,d}, N. PALMIERI⁴, M. PETCU⁵, T. PIEROG¹, H. REBEL¹, M. ROTH¹, H. SCHIELER¹, S. SCHOO⁴, F.G. SCHRÖDER¹, O. SIMA¹², G.C. TRINCHERO⁶, H. ULRICH¹, A. WEINDL¹, J. WOCHOLE¹, J. ZABIEROWSKI¹¹
KASCADE-GRANDE COLLABORATION

¹ Institut für Kernphysik, KIT - Karlsruher Institut für Technologie, Germany

² Universidad Michoacana, Instituto de Física y Matemáticas, Morelia, Mexico

³ Dipartimento di Fisica, Università degli Studi di Torino, Italy

⁴ Institut für Experimentelle Kernphysik, KIT - Karlsruher Institut für Technologie, Germany

⁵ Horia Hulubei National Institute of Physics and Nuclear Engineering, Bucharest, Romania

⁶ Osservatorio Astrofisico di Torino, INAF Torino, Italy

⁷ Universidade São Paulo, Instituto de Física de São Carlos, Brasil

⁸ Fachbereich Physik, Universität Wuppertal, Germany

⁹ Department of Physics, Siegen University, Germany

¹⁰ Dept. of Astrophysics, Radboud University Nijmegen, The Netherlands

¹¹ National Centre for Nuclear Research, Department of Cosmic Ray Physics, Lodz, Poland

¹² Department of Physics, University of Bucharest, Bucharest, Romania

^a now at: Istituto Nazionale di Ricerca Metrologia, INRIM, Torino;

^b now at: Max-Planck-Institut Physik, München, Germany;

^c now at: University of Duisburg-Essen, Duisburg, Germany;

^d now at: University of Trondheim, Norway.

gabriel.toma@nipne.ro

Abstract: The KASCADE-Grande detector is hosted by the Karlsruhe Institute of Technology Campus North, Karlsruhe, Germany and is designed to record showers generated by primaries with an energy in the 10^{16} - 10^{18} eV range. In a standard approach at KASCADE-Grande, the primary energy spectrum has been reconstructed based on a correlation between the muon size and the shower size. We present the result of a second method to reconstruct the primary energy based on another estimator, the charged particle density at 500 m distance from the shower axis, S(500). The S(500)-derived primary energy for recorded events shows a systematic shift from the result of the standard approach, a feature which is not visible when reconstructing simulated events. This shift is larger than the estimated method-specific systematics. We explain this disagreement as mostly an effect caused by the simulations not accurately describing the shape of the lateral density distributions.

Keywords: KASCADE-Grande, primary energy reconstruction, S(500)

1 Introduction

The primary energy of cosmic rays is inferred at KASCADE-Grande [1] using techniques based on different EAS observables. Such techniques are applied independently from each other on the same shower samples (simulated or experimentally recorded showers) and comparison between results is possible. In the standard approach [2] at KASCADE-Grande the primary energy is inferred from the correlation between the total size (N_{ch}) and the muon size (N_{μ}) of the shower. A second approach based on the charged particle density at 500 m from the shower axis - S(500) is described in detail in this paper.

2 KASCADE-Grande

KASCADE-Grande is hosted by the Karlsruhe Institute of Technology - KIT, Campus Nord, Germany (49° N, 8° E) at 110 m a.s.l. It has roughly a rectangular shape with a length

of ≈ 700 m. Historically the KASCADE-Grande detector array is an extension of a smaller array, the KASCADE detector [3]. The extension was guided by the intention to extend the energy range for efficient EAS detection to the energy interval of 10^{16} - 10^{18} eV. The study described in this paper makes use of data recorded by the Grande component, a detector array of 37 scintillator stations with an area of ≈ 10 m² each (Fig. 1).

3 The S(500)

It has been shown that, for a given detector, the charged particle density becomes independent of the primary mass at large fixed radial ranges from the shower axis [4]. For the case of KASCADE-Grande, based on CORSIKA[5]/QGSJet-II [6] simulations, this distance has been found to be 500 m [7] (Fig. 2), hence the notation S(500) for the value of the charged particle density in this

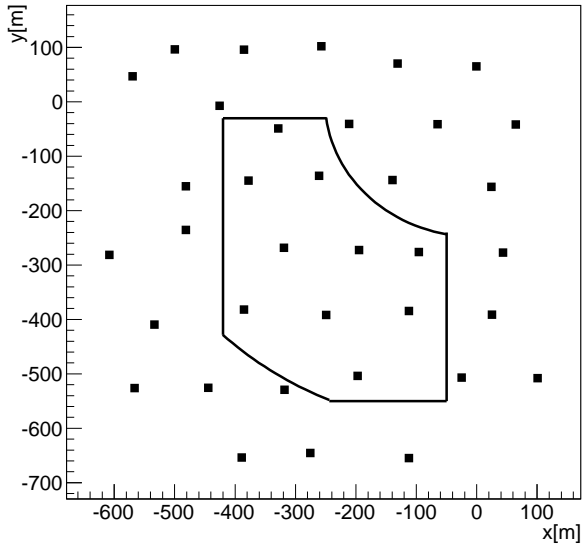


Fig. 1: Schematic top-view of the Grande stations shown as square dots; the fiducial area delimited with line contour is selected as in [2] to facilitate comparison.

particular case.

S(500) is used as a primary energy estimator and the primary energy of recorded events can be reconstructed using a simulation-derived $E_0 - S(500)$ calibration (Fig. 3). The zenith angle distribution is peaked at $\theta \approx 21^\circ$ therefore the calibration curve is derived from events with zenith angles close to this value. Simulations give us also the possibility to test and fine-tune the reconstruction procedure as a whole prior to applying it to real events. Thus the reconstruction is applied identically to both simulated and recorded events.

Before converting the recorded S(500) values into energy we have to account for the variable attenuation of the S(500) in the atmosphere depending on the zenith angle of the shower. This is achieved using the Constant Intensity Cut (CIC) method [8] which is based on the assumption that at full efficiency the same values in the integral fluxes from different zenith angles correspond to the same primary energy. In the frame of the CIC procedure we also evaluate the attenuation length of S(500), $\lambda_{S(500)} = 402 \text{ g}\cdot\text{cm}^{-2}$, by assuming an exponential attenuation pattern for S(500) (Eq. 1).

$$S(500)_\theta = S(500)_{0^\circ} \exp \left[\frac{-h_{0^\circ}}{\lambda_{S(500)}} (\sec\theta - 1) \right] \quad (1)$$

where:

- $S(500)_\theta, S(500)_{0^\circ}$ are the values of S(500) at zenith angles θ and 0° ;
- h_{0° is the atmospheric depth at vertical incidence;
- $\lambda_{S(500)}$ is the attenuation length for S(500).

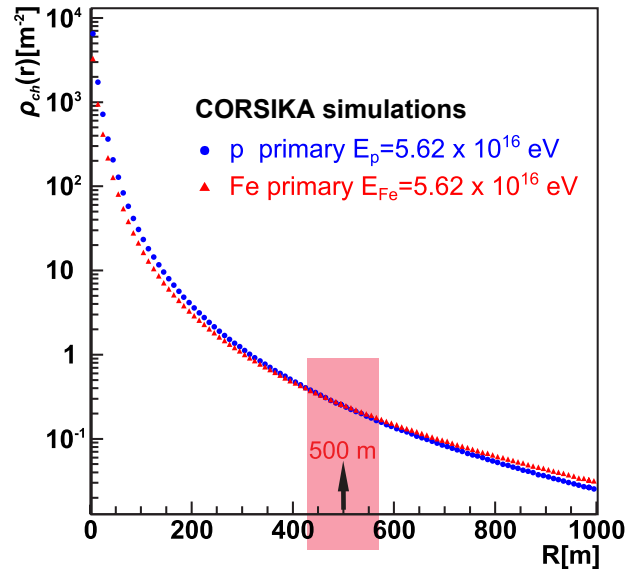


Fig. 2: Averaged simulated lateral distributions for different primary types with equal energy (10 showers simulated for each primary).

4 Results and discussion

Fig. 4 presents the primary energy spectra from KASCADE-Grande (from the described approach based on S(500) and from the standard approach [2]) and the energy spectrum from KASCADE towards lower energies. It is important to note that the KASCADE-Grande spectra and the KASCADE spectrum are obtained with procedures relying on different interaction models (QGSJet-II versus QGSJet01) so the model-specific systematics are not the same. For KASCADE-Grande the S(500)-derived spectrum starts at a higher energy ($\log_{10}(E_0/\text{GeV})=7.5$) than in the standard approach because the full efficiency threshold in the S(500)-based method is reached at higher energies. A single power law fit has a spectral index $\gamma = -3.06 \pm 0.02$ for the S(500)-derived spectrum.

The KASCADE-Grande spectra look similar in shape, but there is a shift between them, larger than the estimated method-specific systematics. The difference between the two methods is visible also in an event-by-event comparison (Fig. 5). At the same time the disagreement does not seem to appear when analysing simulated showers (Fig. 6). This suggests that in fact there is an inconsistency in the way simulations describe real showers (i.e. various observables). Indeed a comparison between simulated and experimental lateral charged particle density distributions (Fig. 7) shows that the data is situated outside the expected (p, Fe) range, towards elements heavier than Fe. Fig. 7 suggests that for a given S(500) the recorded shower size (i.e. integral of the curve) is smaller than the one predicted by simulations. Fig. 8 shows this effect.

We are looking for solutions to bring the simulated events in better agreement with the data such as:

- to decrease the simulated shower size or equivalently to require older showers, one can assume larger interaction cross sections, but this case seems to be discouraged by recent findings [11];
- higher muon multiplicity will increase the curvature

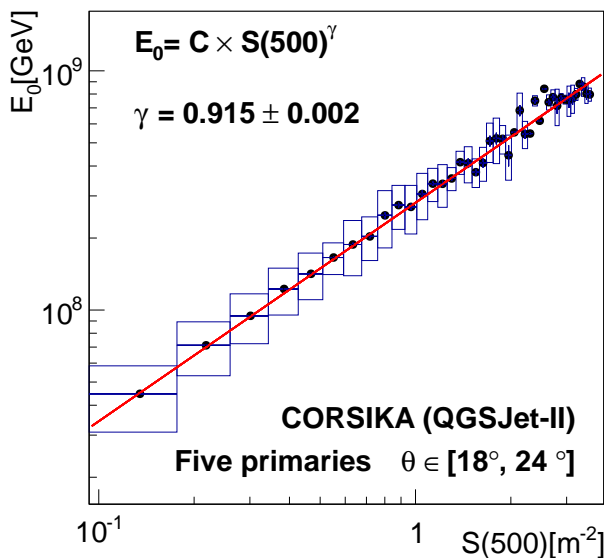


Fig. 3: E_0 - $S(500)$ correlation; the dots are the profile of the scatter plot with box errors showing the spread of data while errors of the mean with simple line are dot sized; the continuous line is a power law fit with $\gamma=0.915\pm 0.002$.

of the simulated lateral distributions as the electron and muon size ratio is not constant over the entire radial range.

5 Conclusions

Two methods have been applied independently at KASCADE-Grande to reconstruct the primary energy for recorded and simulated showers. The results of the two approaches are compared. While for the case of simulations we observe good agreement between reconstructed energy values, for recorded events there is a discrepancy larger than the method-specific systematics. We explain this feature as an effect of simulations not accurately describing the data and we are seeking solutions to improve the agreement between data and simulations.

6 Acknowledgments

The authors would like to thank the members of the engineering and technical staff of the KASCADE-Grande collaboration, who contributed to the success of the experiment. The KASCADE-Grande experiment is supported in Germany by the BMBF and by the 'Helmholtz Alliance for Astroparticle Physics - HAP' funded by the Initiative and Networking Fund of the Helmholtz Association, by the MIUR and INAF of Italy, the Polish Ministry of Science and Higher Education, and the Romanian Authority for Scientific Research UEFISCDI (grants PNII-IDEI 271/2011 and RU-PD 17/2011).

References

[1] W.-D. Apel et al. - KASCADE-Grande Collaboration, Nucl. Instrum. Methods Phys. Res., Sect. A 620 (2010)

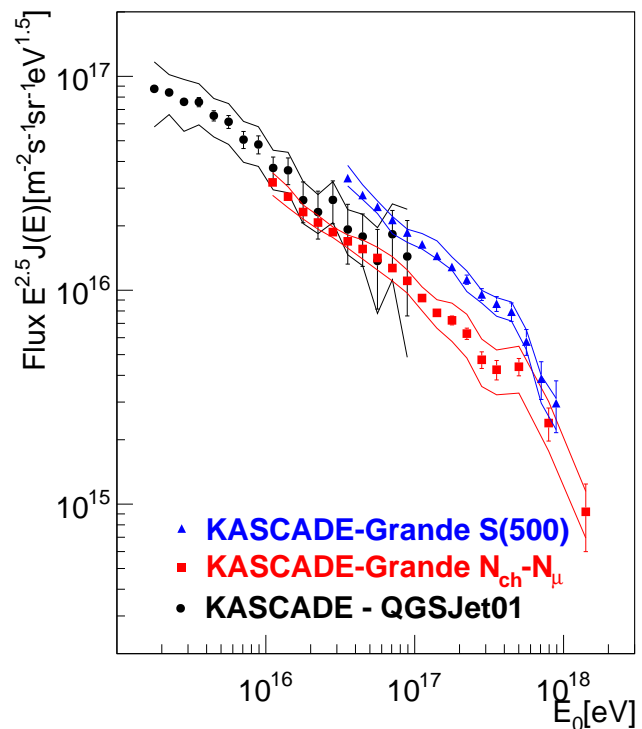


Fig. 4: Primary energy spectra for KASCADE [9] and KASCADE-Grande; the bands with continuous lines show the estimated systematic uncertainty.

202-216 doi:10.1016/j.nima.2010.03.147
 [2] W.-D. Apel et al. - KASCADE-Grande Collaboration, Astroparticle Physics 36 (2012) 183-194 doi:10.1016/j.astropartphys.2012.05.023
 [3] T. Antoni et al. - KASCADE Collaboration, Nucl. Instrum. Methods Phys. Res., Sect. A 513 (2003) 490-510 doi:10.1016/S0168-9002(03)02076-X
 [4] A.M. Hillas et al., Proc.12th ICRC, Hobart 3 (1971) 1001
 [5] D. Heck et al., Report Forschungszentrum Karlsruhe 6019 (1998)
 [6] N.N. Kalmykov, S.S. Ostapchenko and A.I. Pavlov, Nucl. Phys. B (Proc. Suppl.) 52B (1997) 17-28; S.S. Ostapchenko, Nucl. Phys. B-Proc. 151 (2006) 143-147; S.S. Ostapchenko, Phys. Rev. D 74 (2006) 014026
 [7] H. Rebel and O. Sima et al. KASCADE-Grande collaboration, Proc. 29th 612 ICRC Pune India 6 (2005) 297; I.M. Brancus et al. KASCADE-Grande collaboration, Proc. 29th ICRC Pune India 6 (2005) 361
 [8] M. Nagano et al., J.Phys G Nucl.Phys. 10 (1984) 1295
 [9] T. Antoni et al. - KASCADE Collaboration, Astroparticle Physics 24 (2005) 1-25 doi:10.1016/j.astropartphys.2005.04.001
 [10] J. Linsley et al., Journ. Phys. Soc. Japan 17 (1962) A-III
 [11] R. Ulrich et al. - Pierre Auger Collaboration, Phys. Rev. Lett. 109, 062002 (2012); G. Aad et al., ATLAS Collaboration, 2011, arXiv:1104.0326 [hep-ex]. CMS Collaboration, presentation at DIS workshop, Brookhaven, 2011

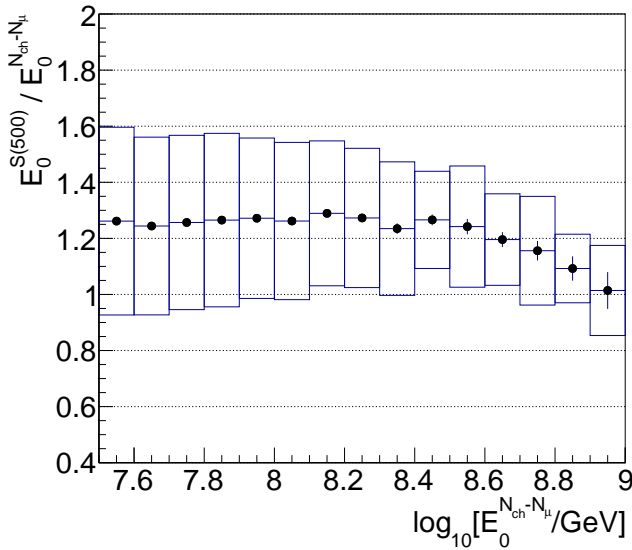


Fig. 5: Ratio between the reconstructed energy in the standard approach, $E_0^{N_{ch}-N_{\mu}}$ and the energy from S(500), $E_0^{S(500)}$; the plot is a profile with box errors showing the spread of data and the bar errors the error of the mean.

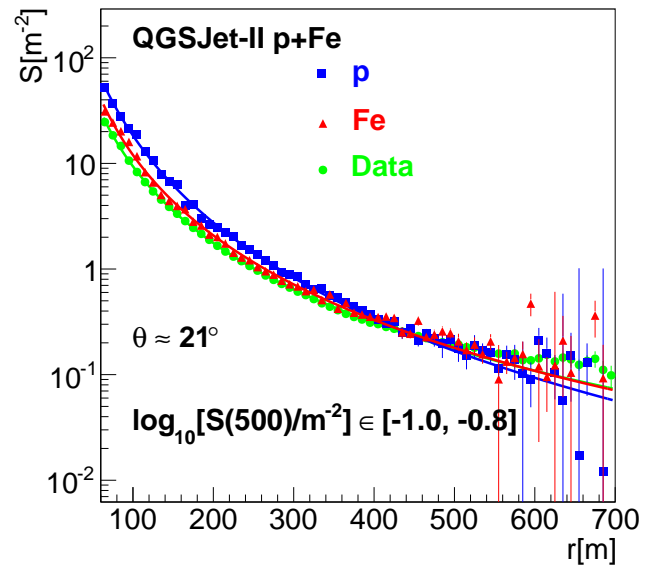


Fig. 7: Averaged lateral charged particle density distributions for simulations (CORSIKA/QGSJet-II p and Fe showers) and experimental data, for events with $\log_{10}[S(500)/m^{-2}] \in [-1, -0.8]$; we show only events inclined at $\approx 21^\circ$ to avoid effects induced by attenuation in the atmosphere; the continuous lines are Linsley [10] fits.

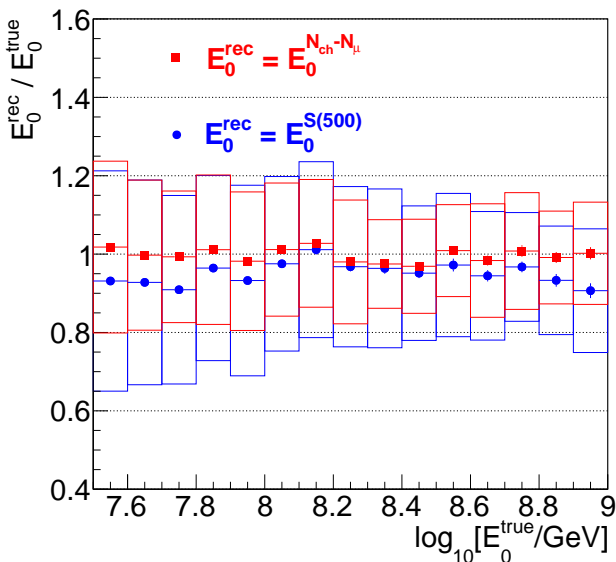


Fig. 6: Event by event representation of the ratio between the reconstructed energy and the true energy as dependence with the primary energy for the two approaches applied on simulated events (five masses in fairly equal proportions); the plots are profiles with the box errors showing the spread of data.

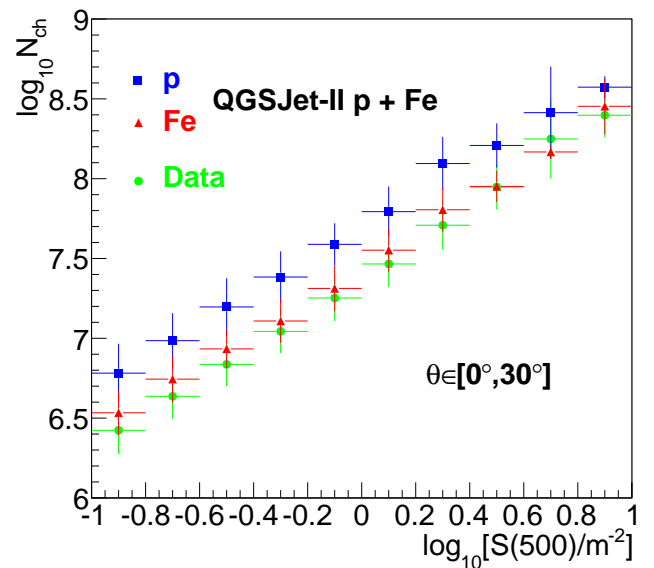


Fig. 8: The correlation between the shower size (as in the standard reconstruction approach) and the S(500) for p and Fe simulated events and for experimental data; the plots are profiles with error bars showing the spread of data.